

Supporting Information for

**Tuning of magnetic properties of the 2D CN-bridged Ni^{II}-Nb^{IV} framework
by incorporation of guest cations of alkali and alkaline earth metals**

Michał Heczko¹, Mateusz Reczyński¹, Christian Näther^{2*}, Beata Nowicka^{1*}

¹ Faculty of Chemistry, Jagiellonian University, Gronostajowa 2, 30-387 Kraków, Poland

² Institut für Anorganische Chemie, Christian-Albrechts-Universität, Max-Eyth.-Str. 2, 24118 Kiel, Germany

Contents:

Figure S1. Powder diffraction patterns of 2 : calculated from SC-XRD model at 170 K, sample in mother liquor, the same sample immersed in pure water for a few days and neutral Ni-Nb network for comparison at room temperature.....	2
Figure S2. Powder diffraction patterns of neutral Ni-Nb compound in water and the same sample immersed in LiCl water solution for 20 days in comparison with data for 1 in mother liquor at room temperature and diffractogram calculated from SC-XRD model at 100 K.....	2
Figure S3. Termogravimetric analysis together with MS scan curves for compounds 1-6	3
Table S1. Continuous Shape Measure parameters for the octa-coordinated niobium centres in compounds 1-6	4
Table S2. Continuous Shape Measure parameters for the hexa-coordinated nickel centres in compounds 1-6	4
Figure S4. Powder X-Ray diffraction patterns at room temperature for crystalline samples 1-6 in mother liquor in comparison with the reference diffractogram of 1 calculated from SC-XRD.	4
Table S3. Selected interatomic distances and bond angles in the structures 1-6	5
Figure S5. Structure of 1 viewed perpendicular to the layers, showing the relative relocation of two neighbouring layers.	6
Figure S6. Asymmetric unit of 1	6
Figure S7. Asymmetric unit of 2	7
Figure S8. Asymmetric unit of 3	7
Figure S9. Asymmetric unit of 4	8
Figure S10. Asymmetric unit of 5	8
Figure S11. Asymmetric unit of 6	9
Figure S12. χ and χT vs. temperature plots in full temperature range at constant magnetic field of 1 kOe.....	10
Figure S13. Magnetic susceptibility measurements on zero-field-cooled and field-cooled samples of 1-6	11
Figure S14. Magnetization vs. magnetic field measurements at 1.8 K with hysteresis parameters (remnant magnetization and coercive field).	12

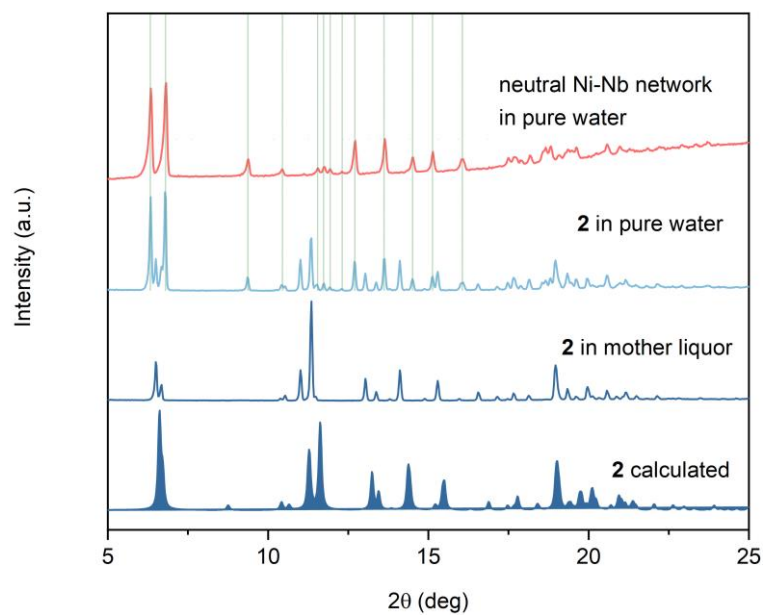


Figure S1. Powder diffraction patterns of **2**: calculated form SC-XRD model at 170 K (bottom), sample in mother liquor, the same sample immersed in pure water for a few days and neutral Ni-Nb network for comparison at room temperature (top).

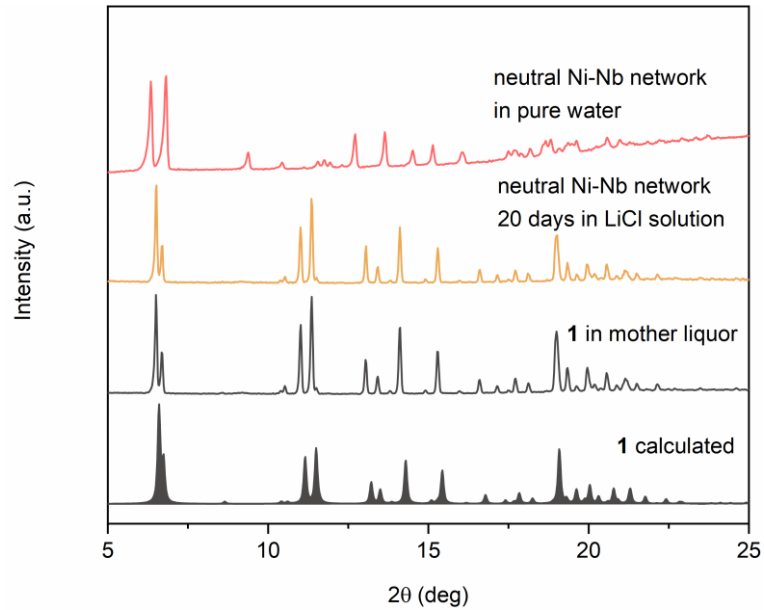


Figure S2. Powder diffraction patterns of neutral Ni-Nb compound in water (top) and the same sample immersed in LiCl water solution for 20 days in comparison with data for **1** in mother liquor at room temperature and diffractogram calculated form SC-XRD model at 100 K (bottom).

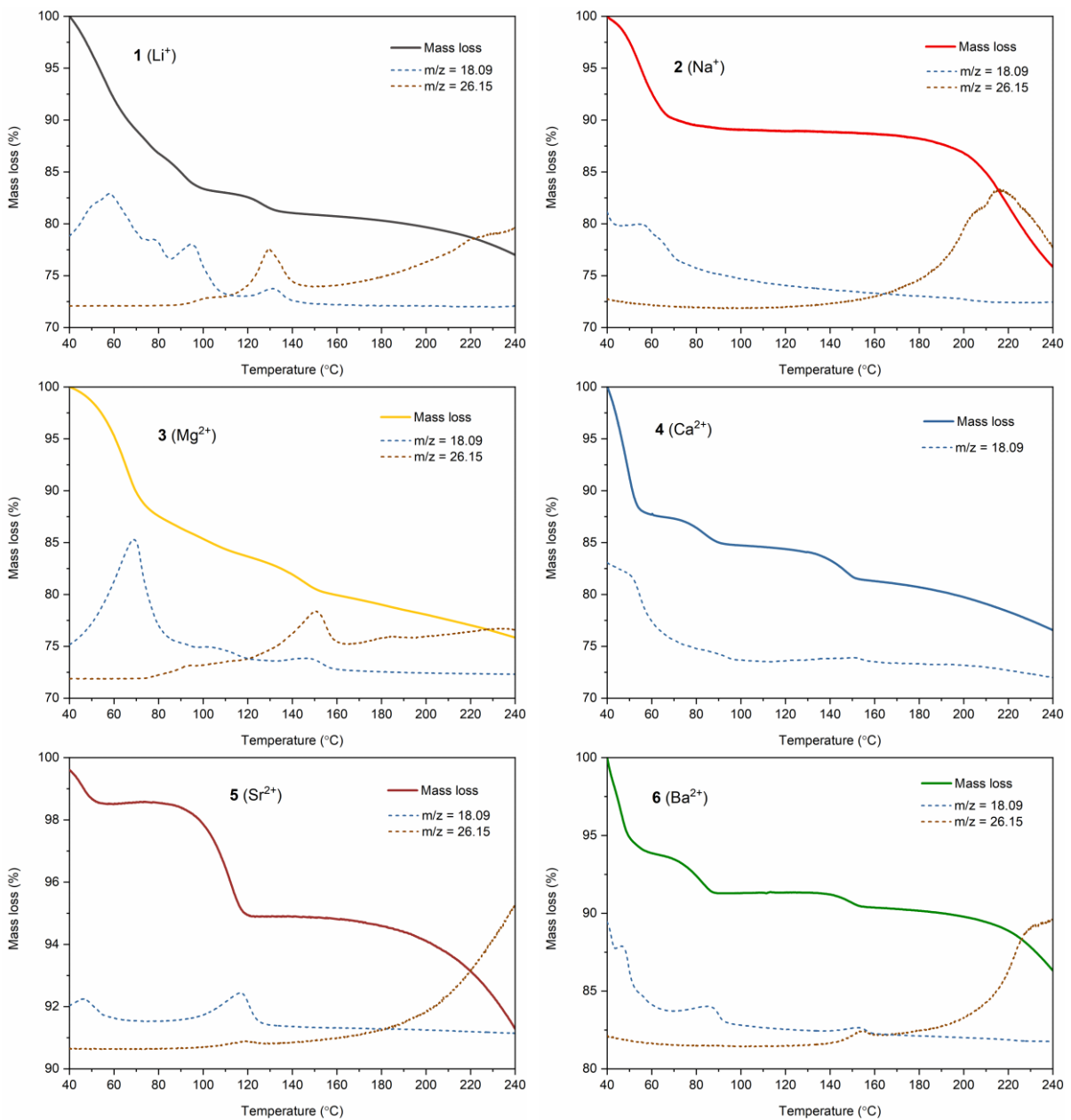


Figure S3. Termogravimetric analysis (solid lines) together with MS scan curves (dashed lines) for compounds **1-6** measured under Ar atmosphere with heating rate of 2°C/min.

Table S1. Continuous Shape Measure parameters for the octa-coordinated niobium centres in compounds **1-6**.

	SAPR-8	TDD-8	BTPR-8	JSD-8
1 Nb1	0.360	1.925	1.214	4.325
2 Nb1	0.354	1.512	1.560	3.940
3 Nb1	0.327	1.714	1.321	4.096
4 Nb1	0.308	1.977	1.331	4.382
5 Nb1	0.319	1.960	1.328	4.376
6 Nb1	0.276	1.485	1.551	3.975
6 Nb2	0.555	1.251	1.214	3.683

CShM = 0 indicates an ideal geometry; SAPR-8 = square antiprism, TDD-8 = triangular dodecahedron, BTPR-8 = biaugmented trigonal prism, JSD-8 = snub disphenoid.

Table S2. Continuous Shape Measure parameters for the hexa-coordinated nickel centres in compounds **1-6**.

1	2	3	4	5	6
Ni1: 0.125	Ni1: 0.192	Ni1: 0.144	Ni1: 0.120	Ni1: 0.143	Ni1: 0.126
Ni2: 0.128	Ni2: 0.118	Ni2: 0.126	Ni2: 0.131	Ni2: 0.142	Ni2: 0.137
OC-6		Ni3: 0.154			Ni3: 0.116
					Ni4: 0.104
					Ni5: 0.196

CShM = 0 indicates an ideal geometry; OC-6 = octahedron.

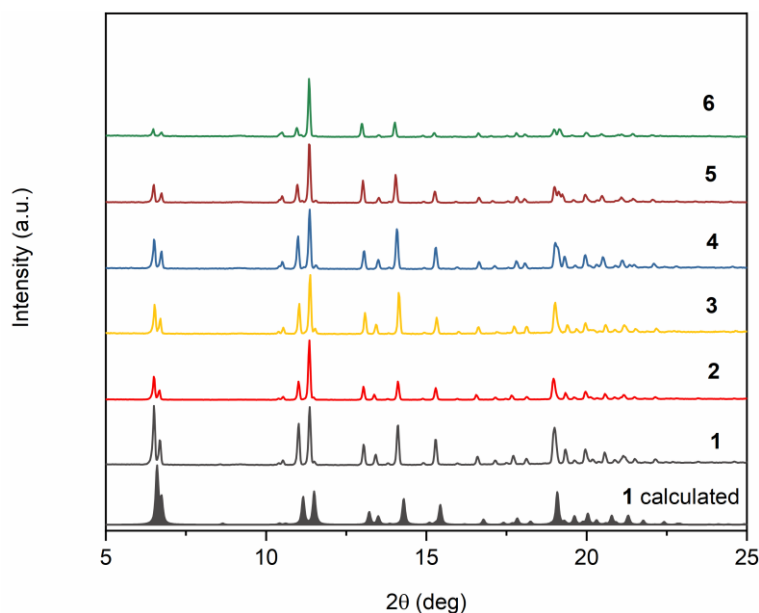


Figure S4. Powder X-Ray diffraction patterns at room temperature for crystalline samples **1-6** in mother liquor in comparison with the reference diffractogram of **1** calculated from SC-XRD.

Table S3. Selected interatomic distances and bond angles in the structures **1-6**.

1 (Li^+)	2 (Na^+)	3 (Mg^{2+})	4 (Ca^{2+})	5 (Sr^{2+})	6 (Ba^{2+})
Distance between metal centres (\AA)					
Ni1-Nb1: 5.2521(5)	Ni1-Nb1: 5.4401(10)	Ni1-Nb1: 5.3791(6)	Ni1-Nb1: 5.2220(14)	Ni1-Nb1: 5.2187(6)	Ni1-Nb1: 5.2489(12)
Ni2-Nb1: 5.3750(4)	Ni2-Nb1: 5.2528(7)	Ni2-Nb1: 5.2459(3)	Ni2-Nb1: 5.3626(9)	Ni2-Nb1: 5.3714(4)	Ni2-Nb1: 5.3458(7)
	Ni3-Nb1: 5.3104(8)				Ni3-Nb1: 5.3712(7)
Ni-N _{CN} distance (\AA)					
Ni1-N1: 2.086(4)	Ni1-N2: 2.130(9)	Ni1-N1: 2.099(3)	Ni1-N2: 2.078(5)	Ni1-N1: 2.074(7)	Ni1-N1: 2.081(7)
Ni2-N2: 2.092(3)	Ni2-N4: 2.097(6)	Ni1-N7: 2.110(3)	Ni2-N1: 2.096(3)	Ni2-N2: 2.093(5)	Ni1-N1A: 2.081(7)
	Ni3-N7: 2.086(7)	Ni2-N2: 2.086(3)			Ni2-N2: 2.062(7)
Ni-N _{cyclam} distance (\AA)					
Ni1-N11: 2.071(4)	Ni1-N11: 2.078(7)	Ni1-N11: 2.071(3)	Ni1-N11: 2.073(4)	Ni1-N11: 2.074(5)	Ni1-N11: 2.069(8)
Ni2-N21: 2.076(6)	Ni1-N12: 2.071(7)	Ni1-N12: 2.079(3)	Ni2-N21: 2.070(4)	Ni2-N21: 2.063(5)	Ni1-N12: 2.071(7)
Ni2-N22: 2.073(7)	Ni2-N21: 2.057(8)	Ni1-N13: 2.068(3)	Ni2-N22: 2.065(4)	Ni2-N22: 2.075(5)	Ni1-N13: 2.089(7)
	Ni2-N22: 2.095(10)	Ni1-N14: 2.076(3)			Ni1-N14: 2.074(7)
	Ni3-N31: 2.082(9)	Ni2-N21: 2.082(3)			Ni2-N21: 2.074(8)
	Ni3-N32: 2.103(9)	Ni2-N22: 2.080(3)			Ni2-N22: 2.071(9)
Ni-N≡C angle ($^\circ$)					
Ni1-N1-C1: 151.4(4)	Ni1-N2-C2: 157.7(7)	Ni1-N1-C1: 159.5(3)	Ni1-N2-C2: 150.9(5)	Ni1-N1-C1: 150.6(6)	Ni1-N1-C1: 151.0(7)
Ni2-N2-C2: 158.7(3)	Ni2-N4-C4: 151.0(6)	Ni1-N7-C7: 157.4(3)	Ni2-N1-C1: 158.5(3)	Ni2-N2-C2: 158.3(4)	Ni1-N1A-C1A: 150.6(7)
	Ni3-N7-C7: 158.5(8)	Ni2-N2-C2: 151.8(2)			Ni2-N2-C2: 159.4(7)
					Ni3-N3-C3: 159.1(6)
					Ni4-N4A-C4A: 156.0(6)
					Ni5-N5A-C5A: 153.0(6)

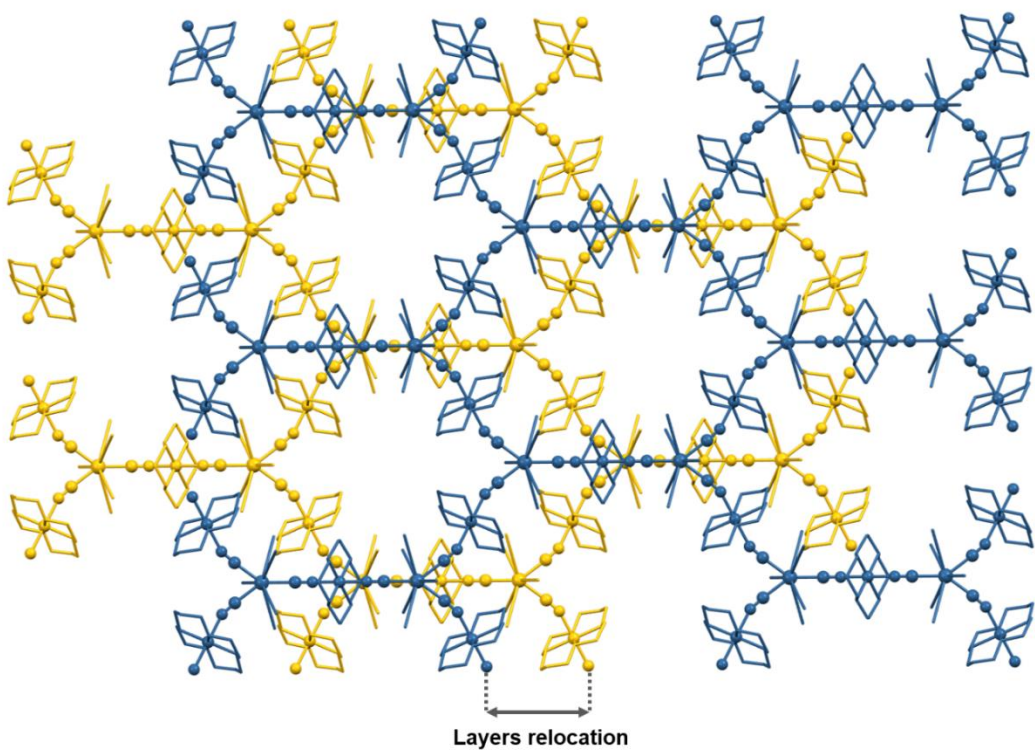


Figure S5. Structure of **1** viewed perpendicular to the layers, showing the relative relocation of two neighbouring layers (water molecules and lithium cations are omitted for clarity).

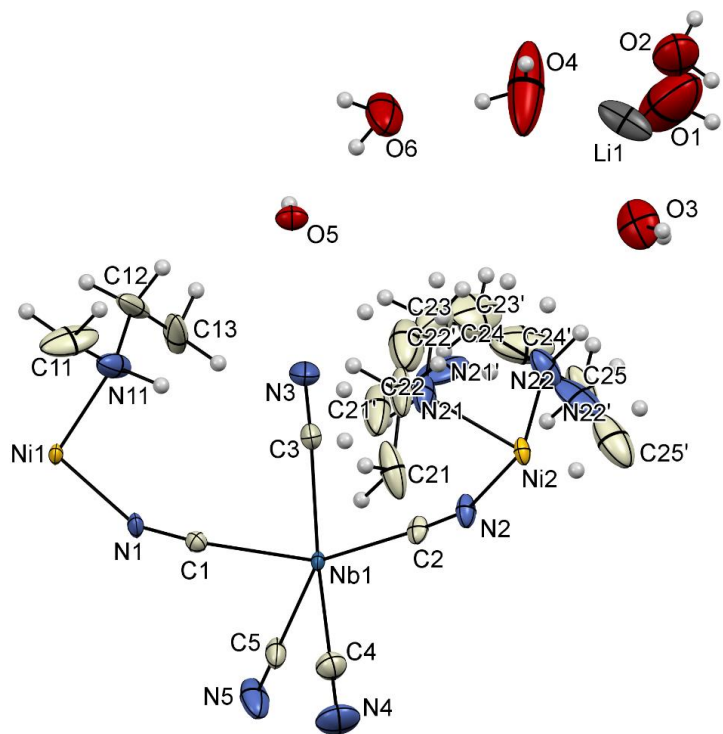


Figure S6. Asymmetric unit of **1**; thermal ellipsoids shown at 50% probability.

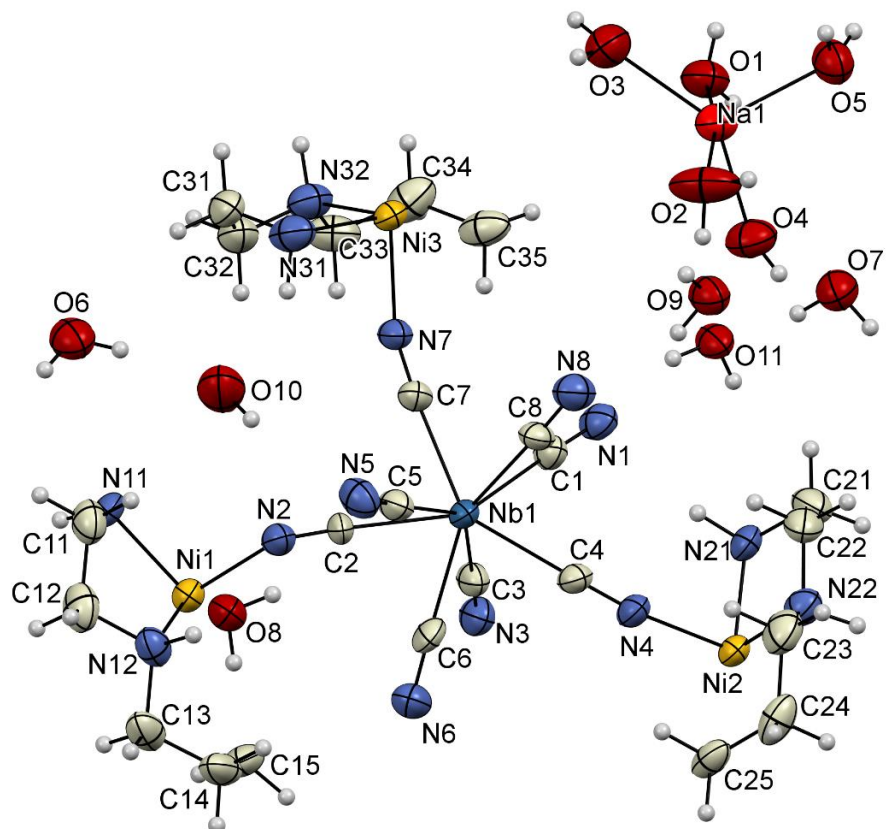


Figure S7. Asymmetric unit of **2**; thermal ellipsoids shown at 50% probability.

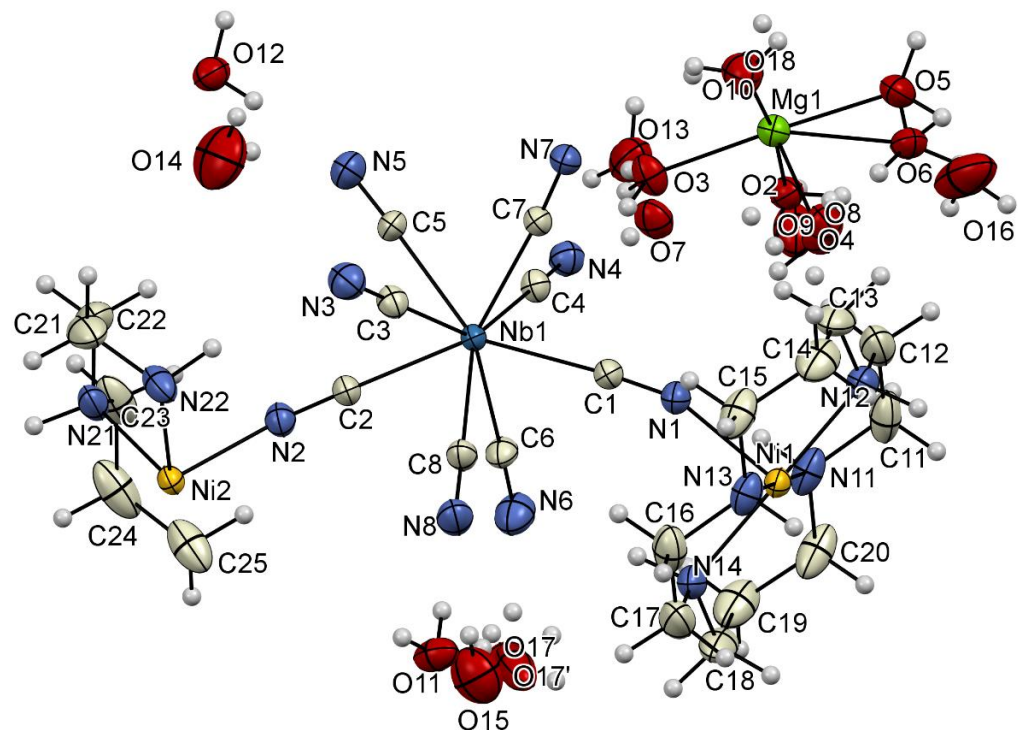


Figure S8. Asymmetric unit of **3**; thermal ellipsoids shown at 50% probability.

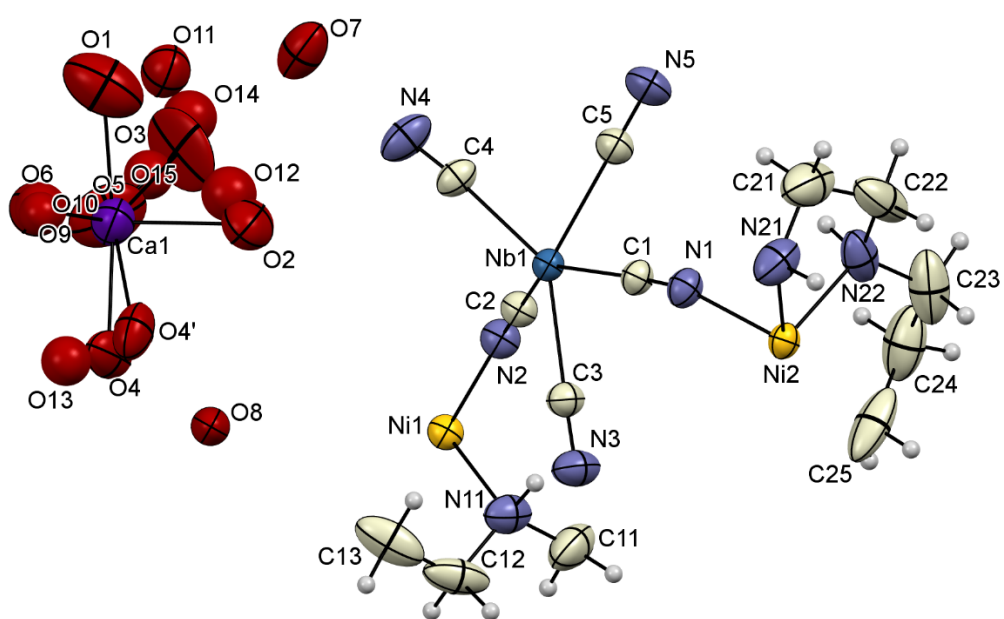


Figure S9. Asymmetric unit of **4**; thermal ellipsoids shown at 50% probability.

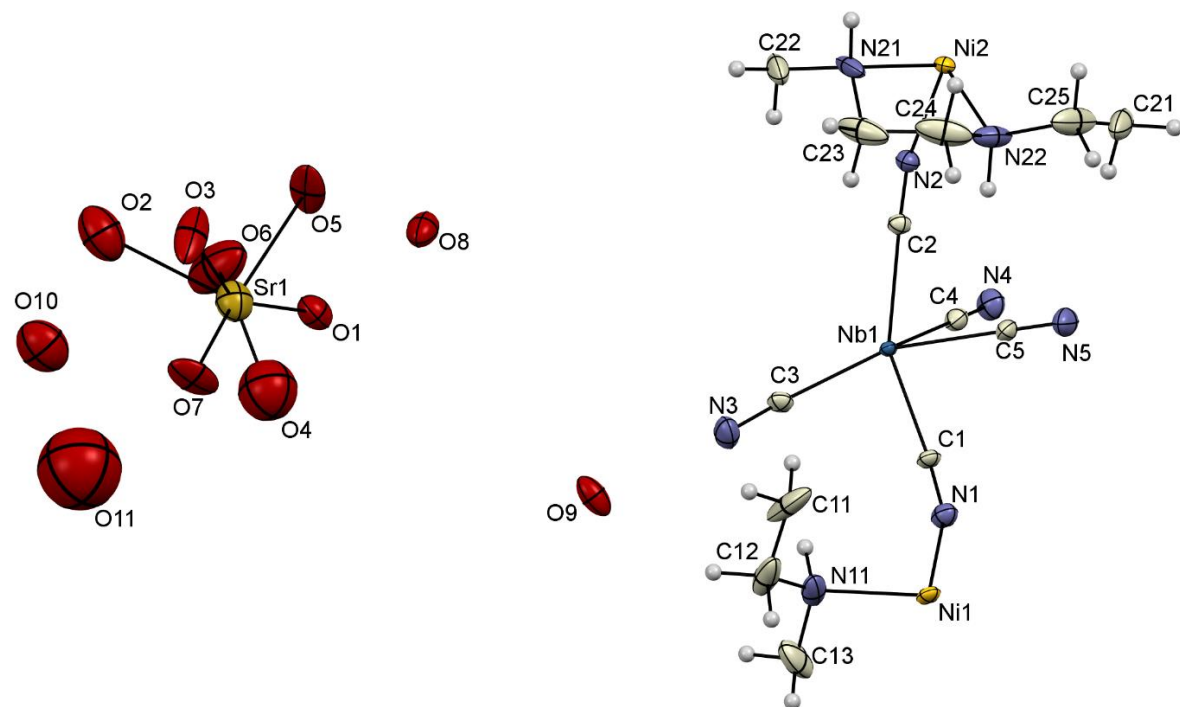


Figure S10. Asymmetric unit of **5**; thermal ellipsoids shown at 50% probability.

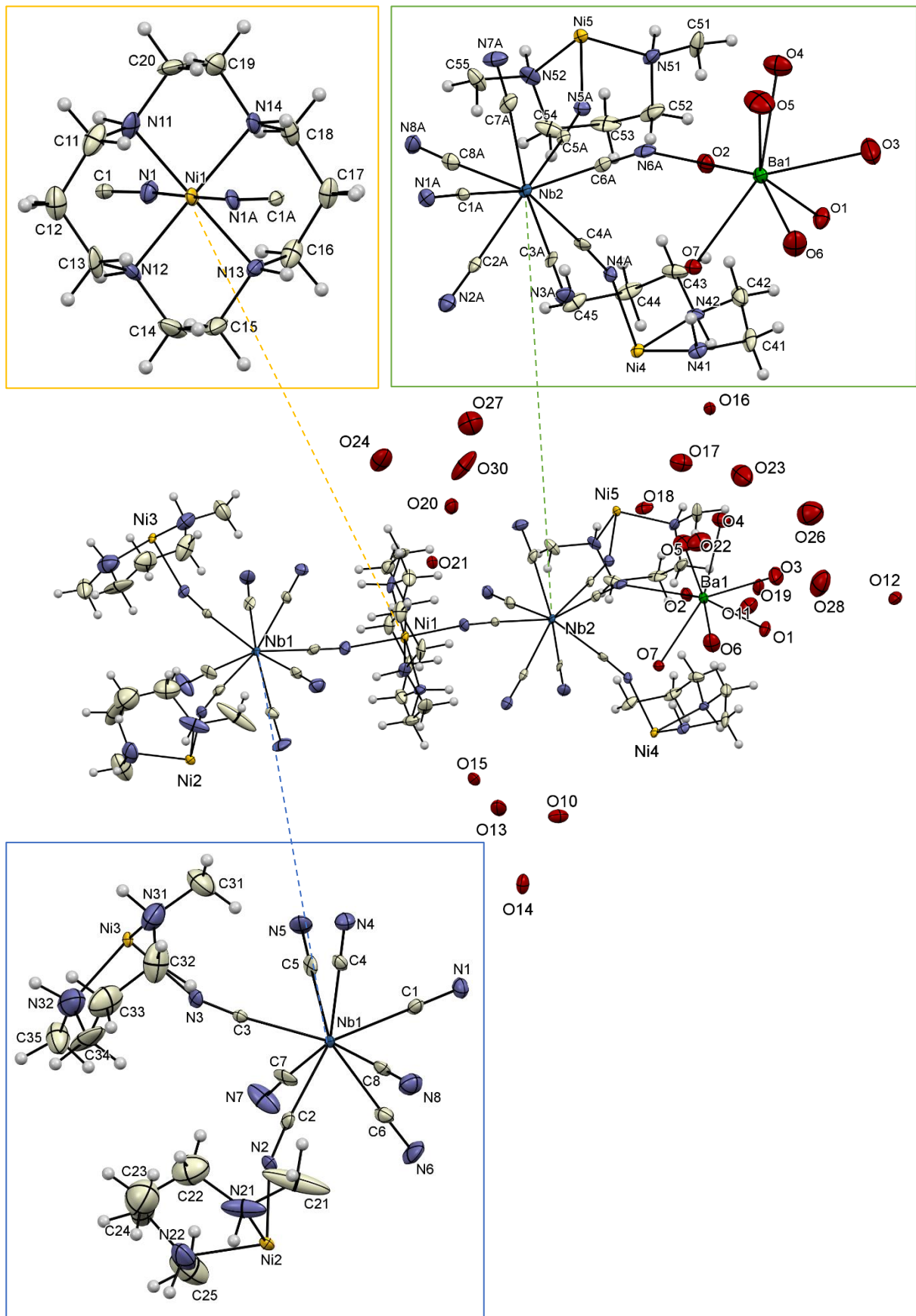
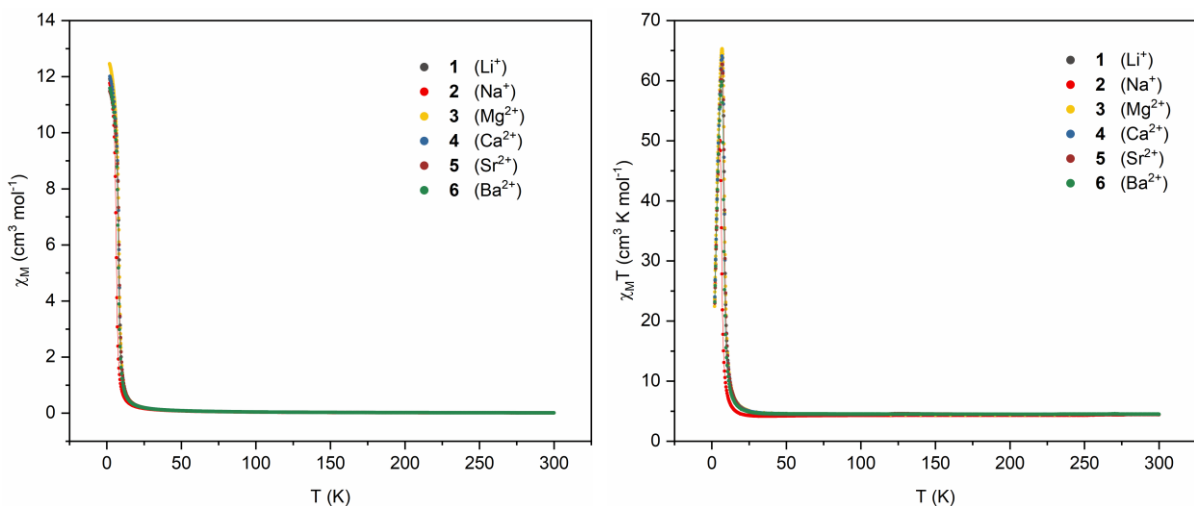
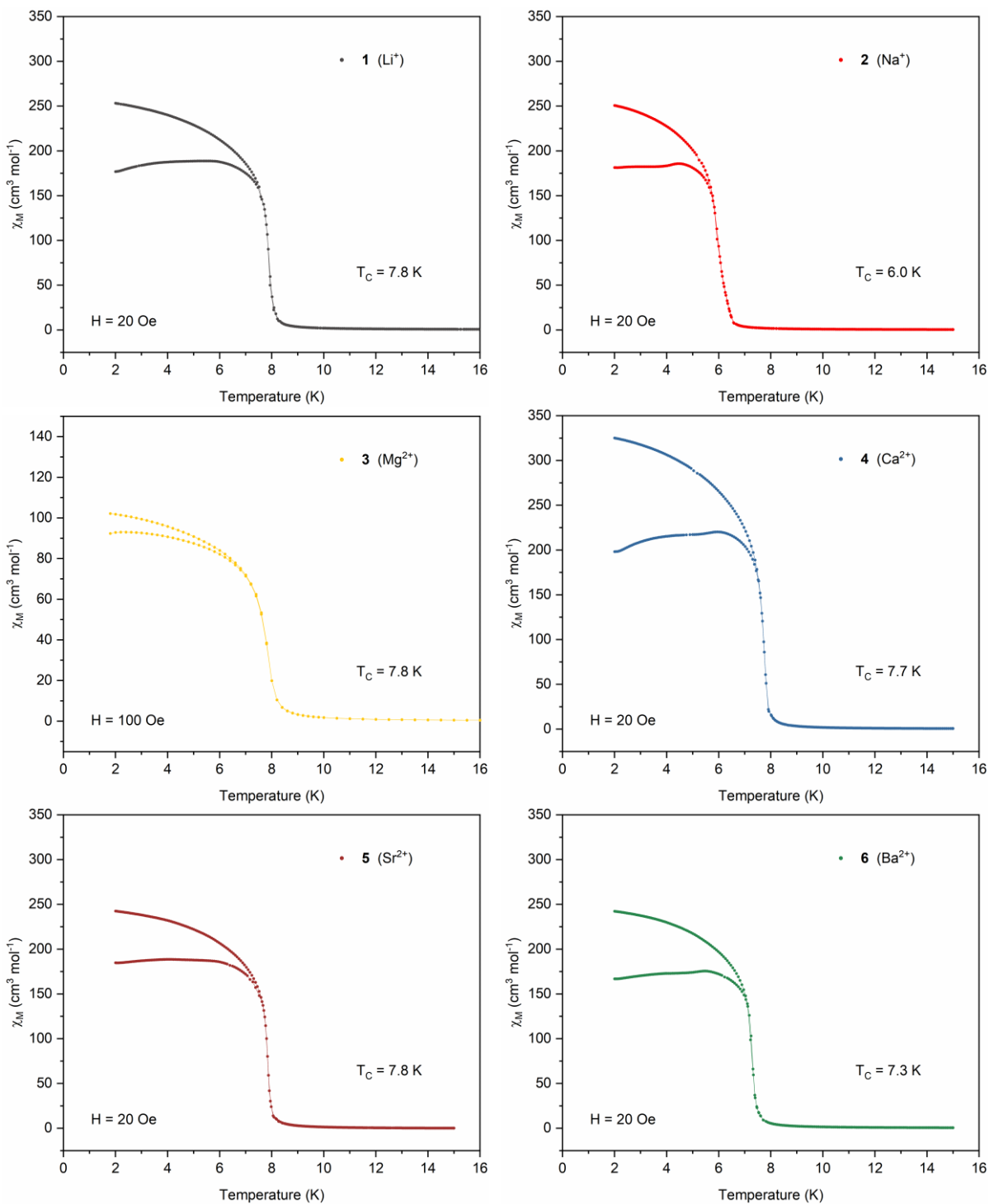


Figure S11. Asymmetric unit of **6**; thermal ellipsoids shown at 50% probability.





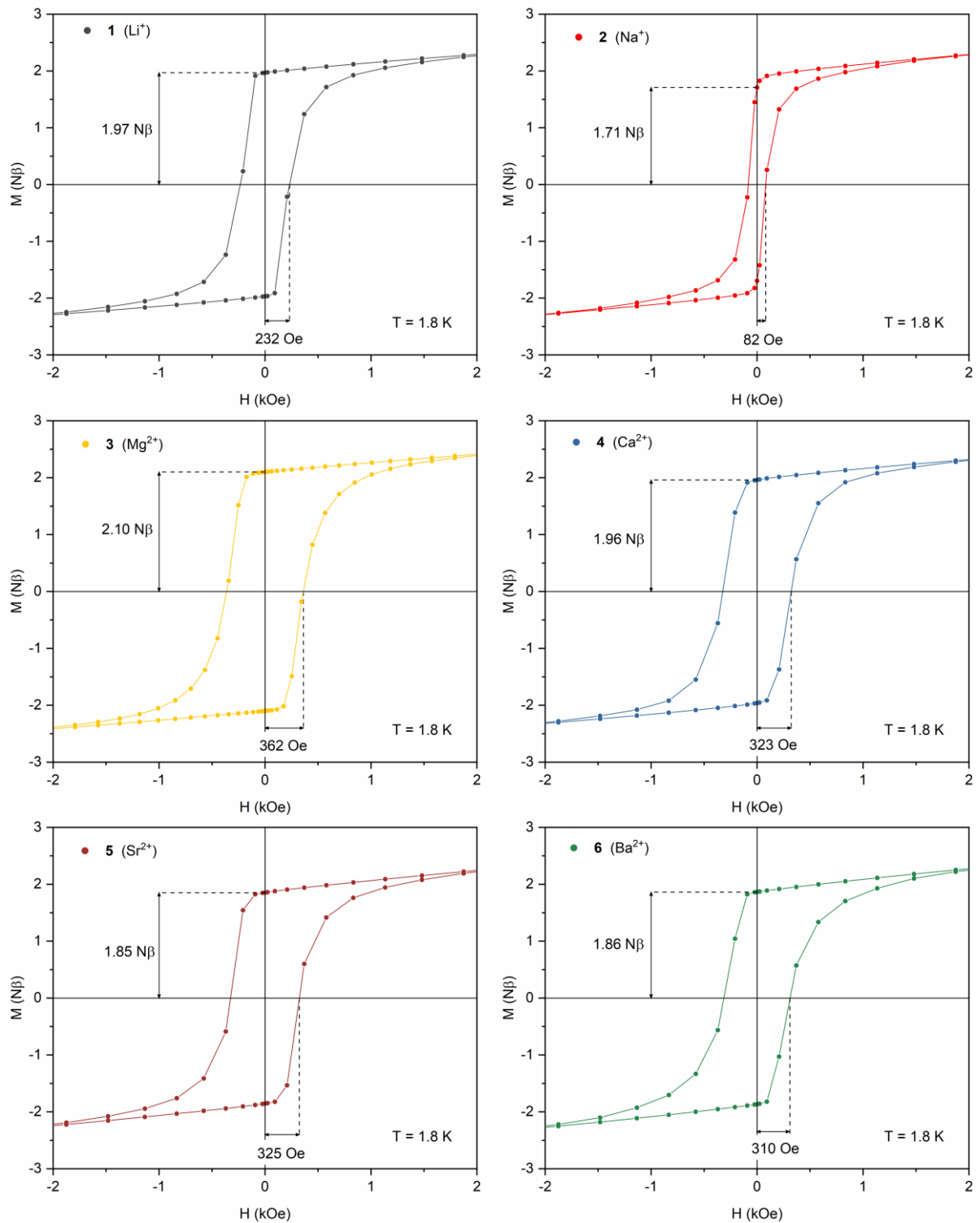


Figure S14. Magnetization vs. magnetic field measurements at 1.8 K with hysteresis parameters (remnant magnetization and coercive field).